

## UvA-DARE (Digital Academic Repository)

### The structure of salt bridges between Arg<sup>+</sup> and Glu<sup>-</sup> in peptides investigated with 2D-IR spectroscopy: Evidence for two distinct hydrogen-bond geometries

Huerta-Viga, A.; Amirjalayer, S.; Domingos, S.R.; Meuzelaar, H.; Rupenyan, A.; Woutersen, S.

**DOI**

[10.1063/1.4921064](https://doi.org/10.1063/1.4921064)

**Publication date**

2015

**Document Version**

Final published version

**Published in**

Journal of Chemical Physics

**License**

CC BY

[Link to publication](#)

**Citation for published version (APA):**

Huerta-Viga, A., Amirjalayer, S., Domingos, S. R., Meuzelaar, H., Rupenyan, A., & Woutersen, S. (2015). The structure of salt bridges between Arg<sup>+</sup> and Glu<sup>-</sup> in peptides investigated with 2D-IR spectroscopy: Evidence for two distinct hydrogen-bond geometries. *Journal of Chemical Physics*, 142(21), Article 212444. <https://doi.org/10.1063/1.4921064>

**General rights**

It is not permitted to download or to forward/distribute the text or part of it without the consent of the author(s) and/or copyright holder(s), other than for strictly personal, individual use, unless the work is under an open content license (like Creative Commons).

**Disclaimer/Complaints regulations**

If you believe that digital publication of certain material infringes any of your rights or (privacy) interests, please let the Library know, stating your reasons. In case of a legitimate complaint, the Library will make the material inaccessible and/or remove it from the website. Please Ask the Library: <https://uba.uva.nl/en/contact>, or a letter to: Library of the University of Amsterdam, Secretariat, P.O. Box 19185, 1000 GD Amsterdam, The Netherlands. You will be contacted as soon as possible.

*UvA-DARE is a service provided by the library of the University of Amsterdam (<https://dare.uva.nl>)*

# The structure of salt bridges between Arg<sup>+</sup> and Glu<sup>-</sup> in peptides investigated with 2D-IR spectroscopy: Evidence for two distinct hydrogen-bond geometries

Adriana Huerta-Viga, Saeed Amirjalayer, Sérgio R. Domingos, Heleen Meuzelaar, Alisa Rupenyan, and Sander Woutersen<sup>a)</sup>

*Van 't Hoff Institute for Molecular Sciences (HIMS), University of Amsterdam, Science Park 904, Amsterdam 1098 XH, The Netherlands*

(Received 4 February 2015; accepted 1 May 2015; published online 18 May 2015)

Salt bridges play an important role in protein folding and in supramolecular chemistry, but they are difficult to detect and characterize in solution. Here, we investigate salt bridges between glutamate (Glu<sup>-</sup>) and arginine (Arg<sup>+</sup>) using two-dimensional infrared (2D-IR) spectroscopy. The 2D-IR spectrum of a salt-bridged dimer shows cross peaks between the vibrational modes of Glu<sup>-</sup> and Arg<sup>+</sup>, which provide a sensitive structural probe of Glu<sup>-</sup> ··· Arg<sup>+</sup> salt bridges. We use this probe to investigate a  $\beta$ -turn locked by a salt bridge, an  $\alpha$ -helical peptide whose structure is stabilized by salt bridges, and a coiled coil that is stabilized by intra- and intermolecular salt bridges. We detect a bidentate salt bridge in the  $\beta$ -turn, a monodentate one in the  $\alpha$ -helical peptide, and both salt-bridge geometries in the coiled coil. To our knowledge, this is the first time 2D-IR has been used to probe tertiary side chain interactions in peptides, and our results show that 2D-IR spectroscopy is a powerful method for investigating salt bridges in solution. © 2015 Author(s). All article content, except where otherwise noted, is licensed under a Creative Commons Attribution 3.0 Unported License. [<http://dx.doi.org/10.1063/1.4921064>]

## I. INTRODUCTION

Salt bridges are hydrogen-bonded ion pairs that play a fundamental role in inter- and intramolecular self-assembly processes. In supramolecular chemistry, salt bridges are used to design new systems.<sup>1-3</sup> Salt bridges also play a role in the intramolecular self assembly (folding) of proteins, where they mediate long-range, tertiary interactions. Salt bridges are a somewhat special case among these interactions, because in many cases it is still not clear whether or not they stabilize the folded conformation of proteins. There is widespread evidence for the presence of salt bridges in stable conformations,<sup>4-7</sup> but the salt-bridge interaction is often found to be energetically unfavorable.<sup>5,8</sup> More importantly, salt bridges can also play a role in the dynamics and functionality of proteins.<sup>9-12</sup> Therefore, a time-resolved structural probe of salt bridges in solution would be a valuable tool to clarify the role that they play in the structure and dynamics of functionally active proteins.

NMR is the standard method to detect salt bridges in solution,<sup>13</sup> but the time resolution of NMR is generally not sufficient to resolve protein dynamics and structural information is not easy to obtain. In the past decade, multi-dimensional vibrational spectroscopy has emerged as a powerful tool to probe the structure of peptides and proteins,<sup>14-18</sup> in particular by probing the amide I' band (which arises from vibrational modes of the backbone) with two-dimensional infrared (2D-IR) spectroscopy.<sup>19-21</sup> The ultrashort pulses used to perform 2D-IR experiments allow a picosecond time resolution for the

dynamics of the system, which makes 2D-IR ideally suited for time-resolved experiments.<sup>22-24</sup> Here, we demonstrate how 2D-IR spectroscopy can be used to detect salt bridges in peptides in solution by investigating the interaction between vibrational modes of arginine (Arg<sup>+</sup>) and glutamate (Glu<sup>-</sup>). We show that as a result of the spatial proximity of the side chains of these amino acids when they form a salt bridge, their local vibrational modes are coupled, and this coupling is directly observable as cross peaks in the corresponding 2D-IR spectrum. We investigate a series of increasingly complex systems where salt bridges between Arg<sup>+</sup> and Glu<sup>-</sup> have a structural function. First, we study an isolated salt bridge between methylguanidinium (MeGdm<sup>+</sup>) and acetate (Ac<sup>-</sup>) to demonstrate that it is possible to detect the salt bridge between Arg<sup>+</sup> and Glu<sup>-</sup> in solution through the off-diagonal response in the 2D-IR spectrum. Subsequently, we study a  $\beta$ -turn peptide that is stabilized by an intramolecular salt bridge between Arg<sup>+</sup> and Glu<sup>-</sup>, an  $\alpha$ -helical peptide that is stabilized by three Arg<sup>+</sup> ··· Glu<sup>-</sup> salt bridges, and a coiled coil whose intra and interhelical (tertiary) structure is stabilized by this type of salt bridges. From the 2D-IR response of these systems we find that in peptides two types of Arg<sup>+</sup> ··· Glu<sup>-</sup> salt bridge occur, with a monodentate and a bidentate hydrogen-bond geometry.

## II. EXPERIMENTAL METHODS

### A. Sample preparations

Methylguanidine·HCl (>98% purity) and tetrabutylammonium acetate (>97% purity) were purchased from Sigma-Aldrich and used without further purification. Hydrogen-deuterium exchange of the carboxyl and guanidinium groups

<sup>a)</sup>Electronic mail: S.Woutersen@uva.nl



of these molecules was achieved by evaporating the compounds from excess D<sub>2</sub>O, and measurements were performed using a 400 mM solution in dimethylsulfoxide (DMSO) at room temperature (23 °C), conditions that ensure more than 90% dimer formation.<sup>25</sup> The  $\beta$ -turn, the  $\alpha$ -helical peptide, and the coiled-coil peptide were custom-synthesized by GL Biochem Ltd. (>95% purity). Remaining trifluoroacetate (TFA) was removed from the  $\alpha$ -helical peptide and the coiled-coil peptide by repeated freeze drying from a 0.1M solution of DCl in D<sub>2</sub>O. In this manner, hydrogen-deuterium exchange of the NH groups was also achieved. The  $\beta$ -turn sample contained a ~100 mM of TFA that was not removed; hydrogen-deuterium exchange was achieved by evaporation from excess D<sub>2</sub>O. TFA has been found to form salt bridges with methylguanidinium,<sup>26</sup> but we found from MD simulations that the presence of TFA in solution with the  $\beta$ -turn does not affect the results presented here.<sup>27</sup> Measurements on the  $\beta$ -turn were done using a 50 mM concentration in DMSO, at room temperature and neutral pD. The  $\alpha$ -helical peptide was measured using a 12 mM concentration in D<sub>2</sub>O, at 2 °C and neutral pD. The coiled-coil peptide was measured using a 25 mM concentration in D<sub>2</sub>O, at 2 °C and neutral pD. To adjust the pD of the samples, aliquots of NaOD or DCl were added. The pD of the  $\beta$ -turn was adjusted in a D<sub>2</sub>O solution and afterwards the sample was freeze-dried and dissolved in DMSO. None of the peptides showed signs of aggregation at the conditions described above. For all measurements, droplets of the solutions were placed between CaF<sub>2</sub> windows (2 mm thick), separated by a teflon spacer of 10–100  $\mu$ m.

### B. 2D-IR measurements

2D-IR spectra were measured with a pump-probe femto-second setup described elsewhere.<sup>28</sup> Briefly, 35 fs pulses (800 nm, 3.2 mJ, 1 kHz) pump an optical parametric amplifier to obtain an approximately Gaussian spectrum centered at ~1580 cm<sup>-1</sup> (16  $\mu$ J, <100 fs, 150 cm<sup>-1</sup> FWHM). This beam is split into pump, probe, and reference beams. The central-frequency of the narrow-band-pump beam is adjusted by means of a Fabry-Perot interferometer (FPI) (~10 cm<sup>-1</sup> FWHM, pulse duration ~1.5 ps). Side maxima in the spectrum transmitted by the FPI are eliminated by using long- and short-pass filters. The sample is pumped with the resulting ~1  $\mu$ J energy. By means of a  $\lambda/2$  plate, the pump beam was rotated 45° with respect to the probe beam. The focal diameter at the pump and probe overlap on the sample was ~200  $\mu$ m, and the pump-probe delay was 1.2 ps. Parallel- and perpendicular-polarization signals were measured by a 90° rotation of a polarizer placed after the sample. We construct the isotropic spectrum from the parallel and perpendicular polarization of pump and probe pulses using the expression  $\Delta\alpha_{\text{iso}} = \frac{1}{3}(\Delta\alpha_{\parallel} + 2\Delta\alpha_{\perp})$ .

### C. *Ab initio* calculations

The geometry-optimization and normal-mode calculations were performed using Gaussian09<sup>29</sup> at the MP2 level of theory using the 6-311+G(d) basis sets.

## III. RESULTS AND DISCUSSION

### A. Isolated salt bridge

We have shown previously that 2D-IR spectroscopy can be used to detect and characterize a salt bridge between guanidinium (Gdm<sup>+</sup>) and Ac<sup>-</sup>.<sup>30</sup> We found that two degenerate CN<sub>3</sub>D<sub>6</sub><sup>+</sup> vibrational modes of Gdm<sup>+</sup>, centered at ~1590 cm<sup>-1</sup>, split up as a result of their coupling with the COO<sup>-</sup> antisymmetric stretch of Ac<sup>-</sup>, which shows a concomitant red shift. When one of the hydrogens of Gdm<sup>+</sup> is substituted by a methyl group, methylguanidinium (MeGdm<sup>+</sup>) is obtained, which is a good model for the side chain of arginine. The methyl substitution breaks the D<sub>3</sub> symmetry of Gdm<sup>+</sup>, and a solvent-independent frequency splitting between its two vibrational modes is induced, resulting in two IR-active modes centered at 1578 cm<sup>-1</sup> and 1608 cm<sup>-1</sup>.<sup>31</sup> Figure 1(d) shows the FTIR spectrum of MeGdm<sup>+</sup> in DMSO, where the above-mentioned bands are visible. These two modes were found to be strongly coupled in Gdm<sup>+</sup>,<sup>30</sup> and a similar coupling is expected for MeGdm<sup>+</sup>. When a salt bridge between MeGdm<sup>+</sup> and Ac<sup>-</sup> is formed, there are two possible geometries in which bidentate hydrogen bonding is possible. The “end-on” geometry, shown in Figure 1(a), involves binding with two NH<sub>2</sub> moieties. The “side-on” geometry, shown in Figure 1(b), involves the methyl-substituted N atom as one of the binding sites. Additionally, there are several possible monodentate binding geometries, one of which is shown in Figure 1(c). It is to be expected that each geometry has different binding strength and, as a consequence, different frequency splittings between the vibrational modes of MeGdm<sup>+</sup> that couple to the Ac<sup>-</sup> mode upon salt-bridge formation. Figure 1(d) shows the infrared absorption spectrum of the MeGdm<sup>+</sup>...Ac<sup>-</sup> dimer in DMSO. The band at 1550 cm<sup>-1</sup> is due to the antisymmetric stretch of the COO<sup>-</sup> moiety of Ac<sup>-</sup>. At higher frequencies there are four bands of MeGdm<sup>+</sup> (indicated with arrows), which we assign to different binding geometries of the dimer. To confirm this assignment, we performed *ab initio* calculations on MeGdm<sup>+</sup>, on the two bidentate binding geometries of the MeGdm<sup>+</sup>...Ac<sup>-</sup> dimer, and on the monodentate geometry of Figure 1(c). The resulting infrared spectra are shown in Figure 1(e). For isolated MeGdm<sup>+</sup> there are two IR-active modes, in agreement with our measurement and previous calculations.<sup>32</sup> The calculated infrared spectra of both bidentate geometries of the MeGdm<sup>+</sup>...Ac<sup>-</sup> dimer consist of three bands. The lowest frequency band at ~1550 cm<sup>-1</sup> corresponds to the COO<sup>-</sup> antisymmetric stretch of Ac<sup>-</sup>. The other two bands correspond to CN<sub>3</sub>D<sub>6</sub><sup>+</sup> modes of MeGdm<sup>+</sup>, both of which are strongly mixed with the COO<sup>-</sup> vibration of Ac<sup>-</sup>. In the calculated spectra, the splitting between the MeGdm<sup>+</sup> and Ac<sup>-</sup> bands is larger for the side-on geometry, which indicates that the coupling strength is larger in this configuration than in the end-on geometry. For both geometries, a value for the coupling between the vibrational modes of MeGdm<sup>+</sup> and Ac<sup>-</sup> is difficult to estimate directly from the changes in the IR frequencies upon salt-bridge formation. This is because these frequency changes are caused not only by the couplings, but also by local-mode frequency changes upon MeGdm<sup>+</sup>...Ac<sup>-</sup> hydrogen bonding. However, in the previously reported Gdm<sup>+</sup>...Ac<sup>-</sup> dimer, for which we

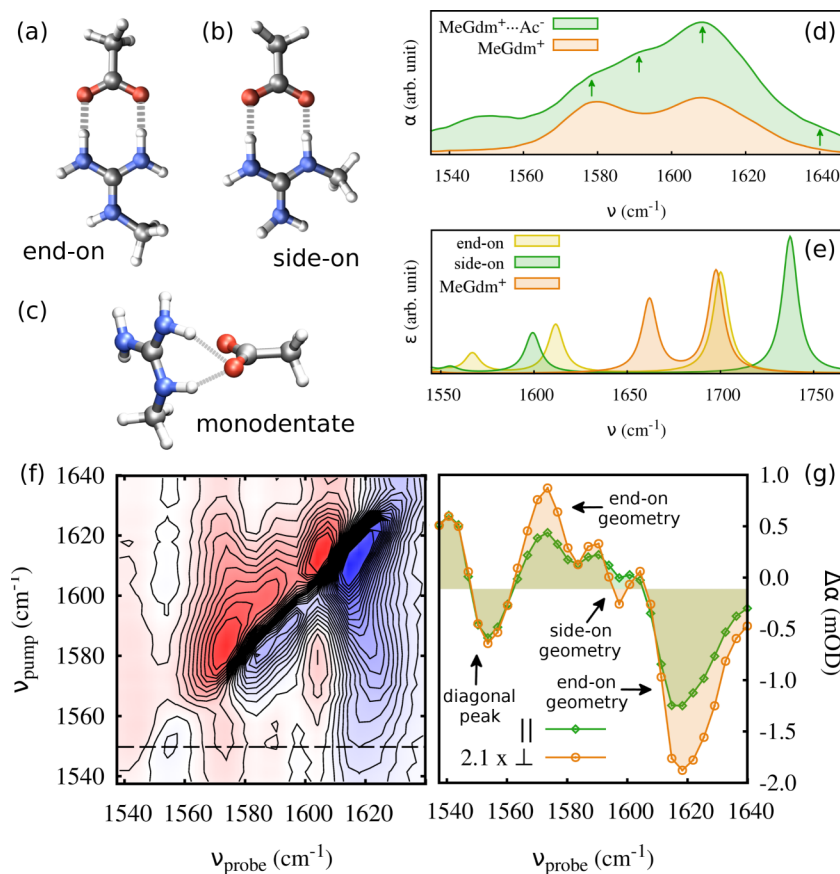


FIG. 1. Molecular picture and infrared response of the MeGdm<sup>+</sup>...Ac<sup>-</sup> dimer. (a) End-on geometry,<sup>7</sup> which allows bidentate binding with two NH<sub>2</sub> moieties. (b) Side-one geometry,<sup>7</sup> which has NH<sub>2</sub> and methyl-substituted N atom as binding sites. (c) One of the possible monodentate geometries, which involves only one oxygen from the carboxylate group of Ac<sup>-</sup>. (d) FTIR spectrum of MeGdm<sup>+</sup> and of the MeGdm<sup>+</sup>...Ac<sup>-</sup> dimer in deuterated DMSO (solvent subtracted). (e) Infrared spectrum obtained from *ab initio* calculations for the two possible bidentate MeGdm<sup>+</sup>...Ac<sup>-</sup> geometries and for isolated MeGdm<sup>+</sup>. (f) 2D-IR spectrum for perpendicular polarization of the pump and probe pulses. The contour intervals are 0.2 m O.D. (g) Scaled cross sections of the parallel and perpendicular 2D-IR spectra for  $\nu_{\text{pump}} = \nu_{\text{Ac}^-}$  (indicated by a dashed line in the 2D plot).

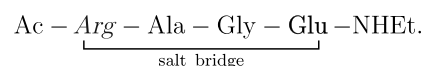
performed a full exciton-model analysis of the 2D-IR spectrum and found couplings with magnitudes of  $\sim 10$  cm<sup>-1</sup>.<sup>30</sup> In the *ab initio* calculation, the monodentate geometry of Figure 1(c) was not a global energy minimum ( $\Delta E > 9$  kcal/mol), and therefore it is probably not significantly populated. However, it is worth noting that in this geometry, the high-frequency MeGdm<sup>+</sup> mode does not show mixing with the COO<sup>-</sup> stretch mode of Ac<sup>-</sup> (see Table S1 in the supplementary material<sup>33</sup> for the atom participation in the normal modes for all geometries).

We measure 2D-IR spectra of MeGdm<sup>+</sup>...Ac<sup>-</sup> solution in DMSO to investigate if the couplings between the modes of MeGdm<sup>+</sup> and Ac<sup>-</sup> predicted by the calculations are observable. Figure 1(f) shows the 2D-IR spectrum of the MeGdm<sup>+</sup>...Ac<sup>-</sup> dimer for perpendicular polarization of pump and probe pulses. The negative absorption changes (blue) along the diagonal are due to the ground-state bleaching plus the  $\nu = 1 \rightarrow 0$  stimulated emission of each of the pumped modes. The positive absorption changes (red) are due to the  $\nu = 1 \rightarrow 2$  induced absorption. When  $\nu_{\text{pump}} = \nu_{\text{Ac}^-}$  (1550 cm<sup>-1</sup>), cross peaks in the off-diagonal region of the 2D-IR spectrum are observed, each consisting of a negative and positive absorption change, at each of the three MeGdm<sup>+</sup> modes in the frequency range probed (the mode with highest frequency is outside this frequency range). A cross section of the 2D-IR spectrum at this pump frequency for parallel and (scaled) perpendicular polarizations is shown in Figure 1(f), where the response of each of the MeGdm<sup>+</sup> modes upon excitation of the Ac<sup>-</sup> mode is seen more clearly. The difference in the intensity ratios of the cross peaks with respect to the diagonal peaks in the parallel and scaled perpendicular cross

sections indicates that the angle between the transition-dipole moments of the coupled modes is nonzero.<sup>34</sup> As mentioned before, the *ab initio* calculation shows that in the side-on geometry there is a larger coupling between the Ac<sup>-</sup> mode and the two MeGdm<sup>+</sup> modes (manifest as a larger frequency splitting). This difference allows us to assign the 1570 cm<sup>-1</sup> and 1605 cm<sup>-1</sup> bands to the end-on geometry, and the 1590 cm<sup>-1</sup> and  $\sim 1640$  cm<sup>-1</sup> bands to the side-on geometry, as indicated in Figure 1(g). The calculation predicts similar extinction coefficients for both binding geometries (see Figure 1(e)), which means that their population can be correlated to their relative intensities in the IR spectra. Additionally, in the 2D-IR spectrum the magnitude of the cross peak is influenced by the magnitude of the diagonal peaks of the coupled modes, and we can conclude that because the MeGdm<sup>+</sup> band at 1590 cm<sup>-1</sup> (assigned to the side-on geometry) is less intense than the other two, the side-on geometry is less populated.

## B. $\beta$ -turn locked by a salt bridge

To investigate if 2D-IR can be used to detect salt bridges in peptides, we first study a  $\beta$ -turn held together by a salt bridge between Arg<sup>+</sup> and Glu<sup>-</sup> when solvated in DMSO.<sup>35</sup> The peptide has the amino acid sequence



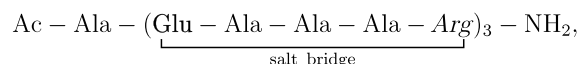
Salt-bridge formation is favored by the flexibility of glycine and alanine, and the fact that the only charges in the molecule

are those of  $\text{Arg}^+$  and  $\text{Glu}^-$ . Isolated  $\text{Arg}^+$  has the same spectrum as  $\text{MeGdm}^+$ , with two IR-active modes centered at  $1578\text{ cm}^{-1}$  ( $\text{Arg}_{\text{LF}}^+$ ) and  $1608\text{ cm}^{-1}$  ( $\text{Arg}_{\text{HF}}^+$ ).<sup>31</sup> In the  $\beta$ -turn, where  $\text{Arg}^+$  forms a salt bridge with the side chain of  $\text{Glu}^-$  (illustrated in Figure 2(a)), the frequency splitting between  $\text{Arg}_{\text{LF}}^+$  and  $\text{Arg}_{\text{HF}}^+$  is larger, as can be seen in the FTIR spectrum of the  $\beta$ -turn shown in Figure 2(b). This larger frequency splitting is already an indication of the existence of an interaction between the vibrational modes of the side chains of  $\text{Arg}^+$  and  $\text{Glu}^-$  in the  $\beta$ -turn. The 2D-IR spectrum unambiguously confirms the existence of a coupling, and hence of a salt bridge, between the side chains of  $\text{Arg}^+$  and  $\text{Glu}^-$ . The isotropic 2D-IR spectrum of the  $\beta$ -turn is shown in Figure 2(c). Along the diagonal the bleach and induced absorption of the carboxylate mode and the two  $\text{Arg}^+$  modes are clearly visible, but their inhomogeneous widths, manifest as the elongation along the diagonal of the 2D-IR spectrum, are larger than in the  $\text{MeGdm}^+ \cdots \text{Ac}^-$  dimer. This indicates a larger conformational variation of the  $\beta$ -turn, probably as a result of the heterogeneity in the backbone conformation of the peptide. In the off-diagonal region there are cross peaks between the two  $\text{Arg}^+$  modes, and also between each of these modes and the  $\text{Glu}^-$  mode. Figure 2(d) shows cross sections for  $\nu_{\text{pump}} = \nu_{\text{Glu}^-}$  (for parallel and perpendicular polarizations of pump and probe pulses), in which the cross peaks between  $\text{Glu}^-$  and both of the  $\text{Arg}^+$  modes are more clearly visible. In the supplementary material Figure S2<sup>33</sup> we show the  $3\Delta\alpha_{\perp} - \Delta\alpha_{\parallel}$  difference spectrum of the  $\beta$ -turn, where all mentioned cross peaks are visible. The cross peaks between the  $\text{Glu}^-$  mode and both of the  $\text{Arg}^+$  modes show that there is a coupling between these modes, and the fact that we are able to measure this coupling for the  $\beta$ -turn shows that we can detect

$\text{Arg}^+ \cdots \text{Glu}^-$  salt bridges in peptides in solution. The 2D-IR response of the  $\beta$ -turn shows only one pair of  $\text{Arg}^+$  bands, indicating that, in contrast to the dimer of Sec. III A, only one salt-bridge geometry occurs. Based on the similarity of the frequencies to the ones in the bidentate dimer, this geometry is most likely the bidentate end-on geometry.

### C. $\alpha$ -helical peptide in aqueous solution

To investigate if 2D-IR can also be used to detect salt bridges in aqueous solution, we studied an  $\alpha$ -helical peptide stabilized by three  $\text{Glu}^- \cdots \text{Arg}^+$  salt bridges.<sup>36</sup> The amino acid sequence of this  $\alpha$ -helical peptide is



and its molecular structure is illustrated in Figure 3(a). The FTIR spectrum of the  $\alpha$ -helical peptide in the  $1550\text{--}1670\text{ cm}^{-1}$  region is shown in Figure 3(b). As before, the lowest-frequency band is due to the  $\text{Glu}^-$  residue. The bands at  $1585$  and  $1605\text{ cm}^{-1}$  are due to the  $\text{Arg}_{\text{LF}}^+$  and  $\text{Arg}_{\text{HF}}^+$  modes, respectively. The band centered at  $1630\text{ cm}^{-1}$  is the amide I' band, whose central frequency is sensitive to the  $\alpha$ -helical content of the peptide. The  $\text{Glu}^-$  band is at a higher frequency than in the  $\text{MeGdm}^+ \cdots \text{Ac}^-$  dimer and the  $\beta$ -turn because of solvation by water.<sup>31</sup> The isotropic 2D-IR spectrum of this peptide is shown in Figure 3(c). The cross peaks between the two  $\text{Arg}^+$  modes are evident, but the cross peaks between these modes and the  $\text{Glu}^-$  mode are difficult to see in the 2D-IR spectrum. However, in a cross section for  $\nu_{\text{pump}} = \nu_{\text{Arg}_{\text{LF}}^+}$ , an off-diagonal response is observed at the frequency of the  $\text{Glu}^-$  mode. This response, although small, has a characteristic bisignate cross-

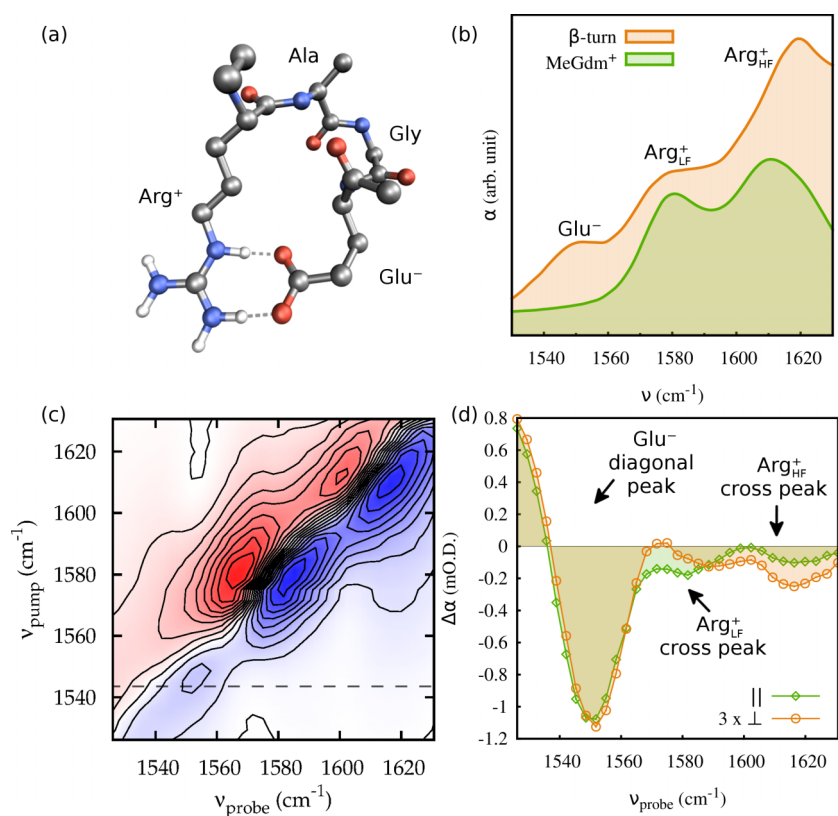


FIG. 2. (a) Molecular representation of the  $\beta$ -turn. (b) FTIR spectrum of  $\text{MeGdm}^+$  and the  $\beta$ -turn in deuterated DMSO (solvent subtracted). (c) Isotropic 2D-IR spectrum of the  $\beta$ -turn. The contour intervals are  $0.3\text{ m.O.D.}$ . (d) Cross sections of the 2D-IR spectra for parallel and (scaled) perpendicular polarizations of pump and probe pulses for  $\nu_{\text{pump}}$  resonant with  $\text{Glu}^-$  (indicated by a dashed line in the 2D plot).

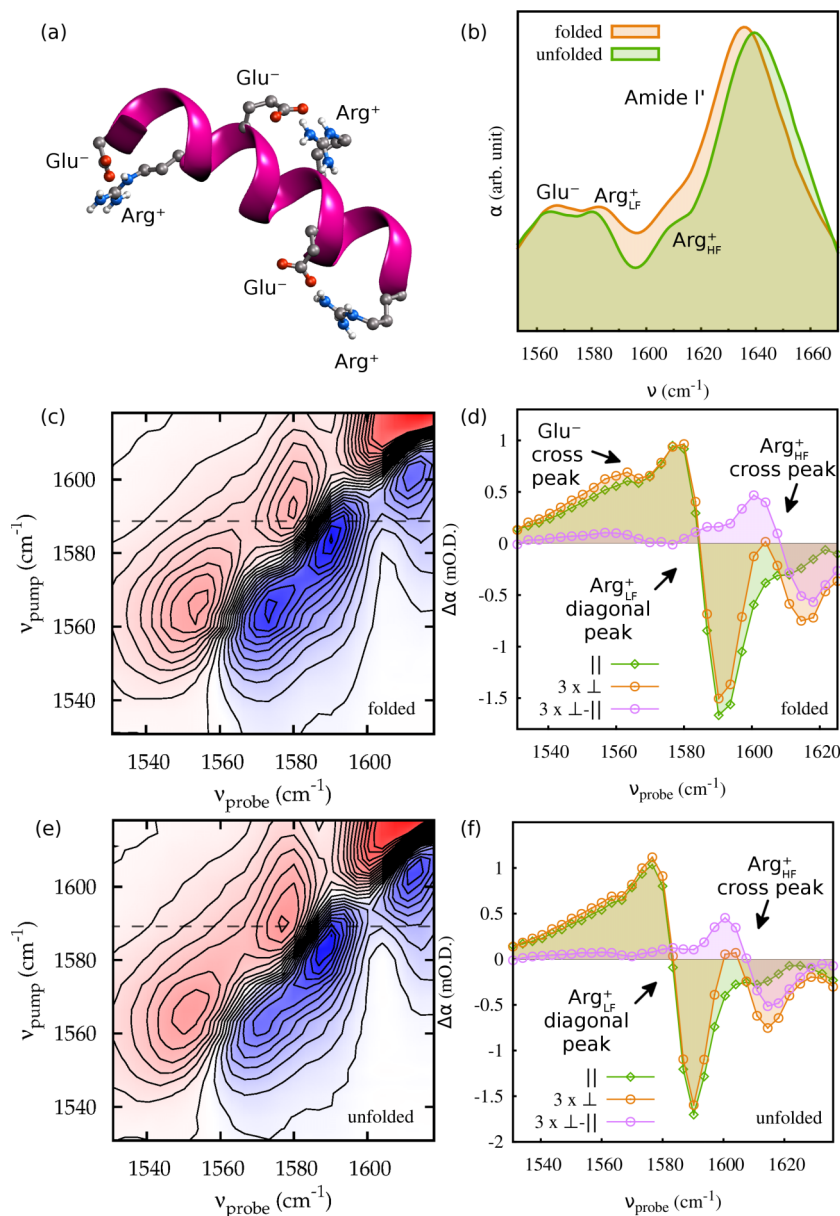


FIG. 3. (a) Molecular representation of the  $\alpha$ -helical peptide. The side chains of Arg<sup>+</sup> and Glu<sup>-</sup> are drawn explicitly. (b) FTIR spectra of the folded and unfolded  $\alpha$ -helical peptide. (c) Isotropic 2D-IR spectrum of the folded peptide. The contour intervals are 0.08 m O.D. (d) Cross sections of the 2D-IR spectra for parallel and (scaled) perpendicular polarizations of pump and probe pulses, and constructed difference for  $\nu_{\text{pump}}$  resonant with Arg<sup>+</sup><sub>LF</sub>. (e) and (f) are the analogous to (c) and (d) for the unfolded  $\alpha$ -helical peptide upon addition of 6M NaCl.

peak line shape and a polarization-dependent magnitude that clearly indicate that it is a cross peak. However, *no* cross peak is observed for  $\nu_{\text{pump}} = \nu_{\text{Arg}^+_{\text{HF}}}$  mode (see supplementary material Figures S3<sup>33</sup> for additional cross sections), which indicates that the Glu<sup>-</sup> mode is only coupled to the Arg<sup>+</sup><sub>LF</sub> mode. This result suggests a monodentate salt-bridge geometry, similar to the one showed in Figure 1(c), for which the Ac<sup>-</sup> mode is only coupled to the low-frequency MeGdm<sup>+</sup> mode. A cross section for  $\nu_{\text{pump}} = \nu_{\text{Glu}^-}$  is not useful for detecting very small Glu<sup>-</sup>/Arg<sup>+</sup><sub>LF</sub> cross peaks because these are overwhelmed by the tail of the diagonal peak of the Arg<sup>+</sup><sub>LF</sub> mode. To confirm that the cross peak between Glu<sup>-</sup> and Arg<sup>+</sup><sub>LF</sub> arises from a salt bridge, we added 6M NaCl to the system, which screens the salt-bridge interaction while disrupting the  $\alpha$ -helical structure of the peptide.<sup>36</sup> Figure 3(b) shows the FTIR spectrum of the unfolded peptide. The amide I' band undergoes a blue shift that is indicative of the loss of  $\alpha$ -helical structure,<sup>37</sup> the Arg<sup>+</sup><sub>LF</sub> mode redshifts and the Glu<sup>-</sup> and Arg<sup>+</sup><sub>HF</sub> modes remain almost unchanged. The off-diagonal region of the

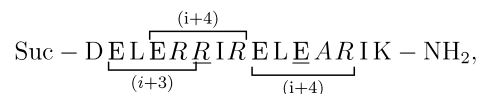
2D-IR spectrum in the salt-bridge region, which is shown in Figure 3(e), provides the explanation for these shifts. The cross peak between Glu<sup>-</sup> and Arg<sup>+</sup><sub>LF</sub> detected for the folded peptide has vanished. This is clearly seen in the cross section for  $\nu_{\text{pump}} = \nu_{\text{Arg}^+_{\text{LF}}}$  mode, shown in Figure 3(f), in which the cross-peak feature at the Glu<sup>-</sup> frequency has disappeared. As a result of the loss of coupling with the Glu<sup>-</sup> side chain, the Arg<sup>+</sup><sub>LF</sub> frequency lowers. The Glu<sup>-</sup> mode also redshifts, but probably because of hydrogen bonding with the surrounding water. These observations prove that the cross peak between Arg<sup>+</sup><sub>LF</sub> and Glu<sup>-</sup> in the folded conformation of the  $\alpha$ -helical peptide arises because of a salt bridge, and the fact that the Glu<sup>-</sup> mode is only coupled to the Arg<sup>+</sup><sub>LF</sub> mode suggests a monodentate rather than a bidentate salt-bridge geometry. To further confirm this structure assignment, we determined the number and relative probability of side-chain rotamers that allow the formation of Glu<sup>-</sup>  $\cdots$  Arg<sup>+</sup> salt bridges in the  $\alpha$ -helical peptide (see supplementary material Figure S6<sup>33</sup> and accompanying text for details). We find that there are three

different accessible rotameric isomers in which salt bridging is possible, and all of them involve only one of the NH groups of the side chain of Arg<sup>+</sup>. This finding supports the presence of a monodentate salt bridge that we detect in the 2D-IR spectra.

#### D. Coiled coil stabilized by salt bridges

Finally, we have investigated if salt bridges stabilizing tertiary structures can be probed with 2D-IR spectroscopy. We studied a coiled coil, a protein structural motif consisting of two or more  $\alpha$ -helical peptides that are wrapped around each other in a superhelical fashion.<sup>38,39</sup> Coiled coils are amongst the most ubiquitous folding motifs found in proteins and have not only been identified in the structure of proteins, but are also involved in various intracellular regulation processes.<sup>40</sup> They are also used as model system to study protein folding and stability due to their small size and because they have both short-range interactions which stabilize the monomeric  $\alpha$ -helices and long-range interactions responsible for oligomeric packing. The coiled-coil peptide that we investigated

was designed *de novo* and characterized before<sup>41</sup> is highly  $\alpha$ -helical and forms 100% dimers in solution under physiological conditions. Its folded conformation is stabilized by a complex network of inter- and intrahelical salt bridges, the most important ones being between Arg<sup>+</sup> and Glu<sup>-</sup>. The peptide has the sequence



where “Suc” at the N-terminus stands for a succinyl group. In Figure 4(a) we show the three-dimensional structure of this peptide obtained with X-ray crystallography.<sup>41</sup> Note that in the crystal, the peptide packs into coiled-coil trimers rather than dimers. In this figure, we show explicitly the side groups of Arg<sup>6+</sup> and Glu<sup>11-</sup> (underlined in the sequence), which are involved in the interhelical salt bridge that stabilizes the coiled coil (for both dimers and trimers). In the crystal structure, the intrahelical salt bridge network shows more structural variability, with many possible salt bridges between Arg<sup>+</sup> and

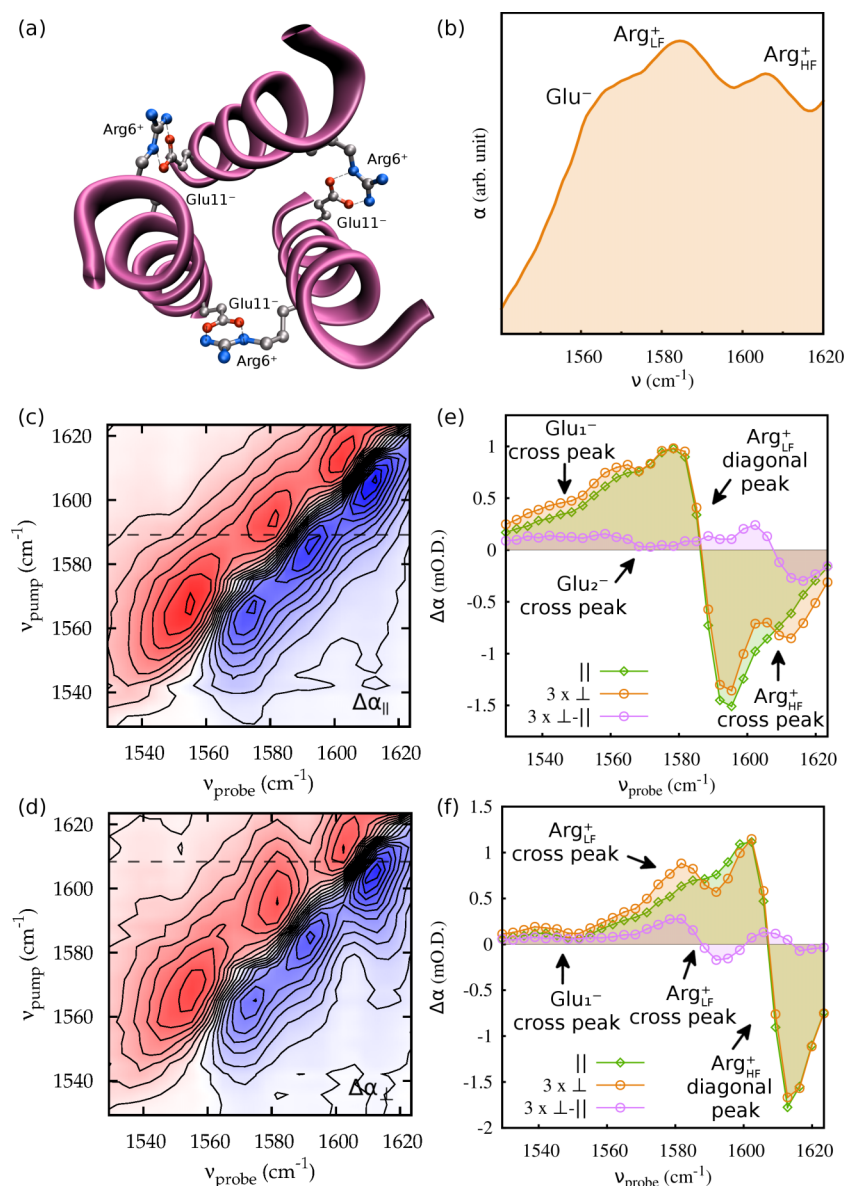


FIG. 4. (a) Molecular representation of the  $\alpha$ -helical coiled coil obtained with X-ray crystallography.<sup>41</sup> The side chains of Arg<sup>6+</sup> and Glu<sup>11-</sup> are drawn explicitly. (b) FTIR spectrum of the coiled coil in D<sub>2</sub>O solution. 2D-IR spectra for (c) parallel, (d) perpendicular polarizations of pump and probe pulses, the contour intervals are 0.17 and 0.06, respectively. Cross sections of the 2D-IR spectra for parallel and (scaled) perpendicular polarizations of pump and probe pulses for  $\nu_{\text{pump}}$  resonant with (e) Arg<sup>6+</sup><sub>LF</sub> and (f) Arg<sup>6+</sup><sub>HF</sub>, indicated by the dashed lines in (c) and (d), respectively.

Glu<sup>-</sup>. It was however found previously that in  $\alpha$  helices salt bridges between Glu<sup>-</sup> and Arg<sup>+</sup> at a distance of four and three residues ( $i + 4$  and  $i + 3$ ) are in general more favorable than those between Arg<sup>+</sup> and Glu<sup>-</sup> (i.e., in reverse order) at the same distance.<sup>36</sup> Hence, in the peptide sequence we only consider the possible Glu<sup>-</sup>...Arg<sup>+</sup> salt bridges with  $i + 4$  and  $i + 3$  spacing. Due to sterical constraints similar to those in the  $\alpha$ -helical peptide, these intrahelical salt bridges are most likely monodentate ones. The Arg6<sup>+</sup>...Glu11<sup>-</sup> interhelical salt bridge lacks these constraints, and might have a different geometry than the intrahelical salt bridges, and therefore a different 2D-IR response. The three-dimensional structure of Figure 4(a) suggests a bidentate geometry for this salt bridge. Figure 4(b) shows the FTIR spectrum of the coiled coil, which as before consists of three bands. The lowest-frequency band arises from the antisymmetric COO<sup>-</sup> stretch of Glu<sup>-</sup>, the other two bands from Arg<sup>+</sup>. The 2D-IR spectra of the coiled coil are shown in Figures 4(c) and 4(d). Along the diagonal, the spectra consist of the three bands that are also visible in the FTIR spectrum, and a weaker response is seen in the off-diagonal region. Cross peaks between the two Arg<sup>+</sup> modes and the Glu<sup>-</sup> mode are better visible in the cross sections shown in Figures 4(e) and 4(f), which consist of cross sections for parallel and perpendicular polarizations of pump and probe pulses, as well as for the weighted difference for  $\nu_{\text{pump}} = \nu_{\text{Arg}_{\text{LF}}^+}$  and  $\nu_{\text{Arg}_{\text{HF}}^+}$ , respectively. The cross section for  $\nu_{\text{pump}} = \nu_{\text{Arg}_{\text{LF}}^+}$  shows two distinctive cross peaks for the Glu<sup>-</sup> mode frequency (labeled Glu<sub>1</sub><sup>-</sup> and Glu<sub>2</sub><sup>-</sup>, as indicated in the figure). The cross section for  $\nu_{\text{pump}} = \nu_{\text{Arg}_{\text{HF}}^+}$  however shows cross peaks only with the Glu<sub>1</sub><sup>-</sup> mode. This observation suggests that there are two different salt-bridge geometries in the coiled coil, giving rise to the two types of 2D-IR response that we detect. In Secs. III A–III C, we showed indications that a salt bridge in which Glu<sup>-</sup> couples to only the Arg<sub>LF</sub><sup>+</sup> mode is a monodentate one (like the  $\alpha$ -helical peptide presented in Sec. III C), whereas a salt bridge in which Glu<sup>-</sup> couples to both Arg<sup>+</sup> modes is a bidentate one (and as a result shifting to a lower frequency due to the stronger coupling, similarly to what we observed for the  $\beta$ -turn). Hence, the Glu<sub>2</sub><sup>-</sup> mode, which is coupled only to the Arg<sub>LF</sub><sup>+</sup> mode, indicates a monodentate salt-bridge geometry, very likely to occur in the intrahelical salt bridges (highlighted in the peptide sequence) that adopt this geometry due to sterical constraints imposed by the helical structure of the backbone. The Glu<sub>1</sub><sup>-</sup> mode of Figure 4(e), which is coupled to both Arg<sup>+</sup> modes, indicates a bidentate salt bridge, most likely the interhelical Arg6<sup>+</sup>...Glu11<sup>-</sup> salt bridge, in agreement with the molecular representation of Figure 4(a). In the supplementary material Figure S5<sup>33</sup> we show cross sections for  $\nu_{\text{pump}}$  resonant with Glu<sub>1</sub><sup>-</sup> and Glu<sub>2</sub><sup>-</sup> frequencies. The two different Glu<sup>-</sup> modes cannot be distinguished along the diagonal because their separation is about 15 cm<sup>-1</sup>, which is most likely less than their inhomogeneous widths. Furthermore, there is only one Glu<sub>1</sub><sup>-</sup> group and three Glu<sub>2</sub><sup>-</sup> groups per helix in the coiled coil, so that the diagonal peak of the former is much less intense than that of the latter.

To determine if excitation transfer contributes to the observed cross peaks, we investigated the intensity of the cross peaks as a function of delay between pump and probe pulses

for  $\nu_{\text{pump}} = \nu_{\text{Arg}_{\text{HF}}^+}$  (see supplementary material Figure S7<sup>33</sup>). We find that the cross peak between the two Arg<sup>+</sup> increases with waiting time, in agreement with previous results.<sup>32</sup> We also find that the Glu<sub>1</sub><sup>-</sup> cross peak has a larger relative intensity at longer delays, which indicates that the Arg<sub>HF</sub><sup>+</sup>/Glu<sup>-</sup> cross peaks are caused by both coherent coupling and excitation transfer. The intensities of the cross peaks at 1.2 ps delay can therefore not be related directly to vibrational cross anharmonicities. At short delay, this assignment might be possible, but our experimental configuration does not allow such measurement because of the duration of our narrow-band pump pulse.

#### IV. CONCLUSION

We have shown that 2D-IR spectroscopy is a robust and widely applicable probe of salt bridges. We use this probe to detect the salt bridge in solution between Arg<sup>+</sup> and Glu<sup>-</sup> in a dimer, a  $\beta$ -turn, an  $\alpha$ -helical peptide, and a coiled coil. We can distinguish salt bridges with different hydrogen-bond geometries: bidentate geometries are present in the dimer and the  $\beta$ -turn, a monodentate geometry is present in the  $\alpha$ -helical peptide, and both geometries are present in the coiled coil. The monodentate geometry arises most likely due to sterical constraints that restrict the intrinsically preferred rotameric conformations of the side chains involved in the salt bridge. 2D-IR spectroscopy can also be used to study salt bridges in larger peptides and proteins, since intrinsic complications such as spectral crowding can be overcome by using isotopic labels: <sup>15</sup>N for Arg<sup>+</sup> (~40 cm<sup>-1</sup> redshift)<sup>42</sup> and <sup>18</sup>O for Glu<sup>-</sup> (~10 cm<sup>-1</sup> redshift).<sup>43</sup>

The results presented here demonstrate a method for probing salt bridges in solution with picosecond time resolution, that is ideally suited for time-resolved experiments to investigate systems in which salt bridges are structurally or functionally relevant. Such detection and characterization of salt bridges in solution should bring new insights into the controversial role that they play in the structure, folding dynamics, and biochemical functioning of proteins.

#### ACKNOWLEDGMENTS

The authors thank W. J. Buma for critically reading this manuscript. This work was financially supported by the Netherlands Organisation for Scientific Research (NWO). S.A. would like to thank the Deutsche Akademie der Naturforscher Leopoldina–German National Academy of Sciences for a Leopoldina research fellowship (Grant No. LPDS 2011-18). S.R.D. acknowledges financial support from the Portuguese Foundation for Science and Technology (FCT) under the fellowship SFRH/BD/48295/2008. S.W., A.R., and H.M. acknowledge the European Research Council (ERC) for funding through Grant No. 210999.

<sup>1</sup>M. Ikeda, Y. Tanaka, T. Hasegawa, Y. Furusho, and E. Yashima, *J. Am. Chem. Soc.* **128**, 6806–6807 (2006).

<sup>2</sup>B. Kuberski and A. Szumna, *Chem. Commun.* **2009**, 1959–1961.

<sup>3</sup>L. E. R. O’Leary, J. A. Fallas, E. L. Bakota, M. K. Kang, and J. D. Hartgerink, *Nat. Chem.* **3**, 821–828 (2011).

- <sup>4</sup>J. Singh, J. Thornton, M. Snarey, and S. Campbell, *FEBS Lett.* **224**, 161–171 (1987).
- <sup>5</sup>S. Kumar and R. Nussinov, *J. Mol. Biol.* **293**, 1241–1255 (1999).
- <sup>6</sup>K. D. Walker, T. P. Causgrove, and R. T. Sauer, *J. Mol. Model.* **15**, 1213–1219 (2009).
- <sup>7</sup>J. E. Donald, D. W. Kulp, and W. F. DeGrado, *Proteins* **79**, 898–915 (2011).
- <sup>8</sup>C. D. Waldburger, J. F. Schildbach, and R. T. Sauer, *Nat. Struct. Biol.* **2**, 122–128 (1995).
- <sup>9</sup>L. Cruz, B. Urbanc, J. M. Borreguero, N. D. Lazo, D. B. Teplow, and H. E. Stanley, *Proc. Natl. Acad. Sci. U. S. A.* **102**, 18258–18263 (2005).
- <sup>10</sup>A. Moroni and G. Thiel, *Nat. Chem. Biol.* **2**, 572–573 (2006).
- <sup>11</sup>J. M. Christie, A. S. Arvai, K. J. Baxter, M. Heilmann, A. J. Pratt, A. O'Hara, S. M. Kelly, M. Hothorn, B. O. Smith, K. Hitomi, G. I. Jenkins, and E. D. Getzoff, *Science* **335**, 1492–1496 (2012).
- <sup>12</sup>H. Meuzelaar, M. Tros, A. Huerta-Viga, C. N. van Dijk, J. Vreede, and S. Woutersen, *J. Phys. Chem. Lett.* **5**, 900–904 (2014).
- <sup>13</sup>P. Strop and S. L. Mayo, *Biochemistry* **39**, 1251–1255 (2000).
- <sup>14</sup>W. Zhuang, T. Hayashi, and S. Mukamel, *Angew. Chem., Int. Ed.* **48**, 3750–3781 (2009).
- <sup>15</sup>J. Jeon, S. Yang, J. H. Choi, and M. Cho, *Acc. Chem. Res.* **42**, 1280–1289 (2009).
- <sup>16</sup>F. Fournier, R. Guo, E. M. Gardner, P. M. Donaldson, C. Loefffeld, I. R. Gould, K. R. Willison, and D. R. Klug, *Acc. Chem. Res.* **42**, 1322–1331 (2009).
- <sup>17</sup>M. C. Thielges, J. K. Chung, and M. D. Fayer, *J. Am. Chem. Soc.* **133**, 3995–4004 (2011).
- <sup>18</sup>J. N. Bandaria, S. Dutta, M. W. Nydegger, W. Rock, A. Kohen, and C. M. Cheatum, *Proc. Natl. Acad. Sci. U. S. A.* **107**, 17974–17979 (2010).
- <sup>19</sup>P. Hamm, M. Lim, W. F. DeGrado, and R. M. Hochstrasser, *Proc. Natl. Acad. Sci. U. S. A.* **96**, 2036–2041 (1999).
- <sup>20</sup>N. Demirdöven, C. M. Cheatum, H. S. Chung, M. Khalil, J. Knoester, and A. Tokmakoff, *J. Am. Chem. Soc.* **126**, 7981–7990 (2004).
- <sup>21</sup>Z. Ganim, H. S. Chung, A. W. Smith, L. P. DeFlores, K. C. Jones, and A. Tokmakoff, *Acc. Chem. Res.* **41**, 432–441 (2008).
- <sup>22</sup>A. Stolow and D. M. Jonas, *Science* **305**, 1575–1577 (2004).
- <sup>23</sup>C. Kolano, J. Helbing, M. Kozinski, W. Sander, and P. Hamm, *Nature* **444**, 469–472 (2006).
- <sup>24</sup>V. Cervetto, P. Hamm, and J. Helbing, *J. Phys. Chem. B* **112**, 8398–8405 (2008).
- <sup>25</sup>B. Linton and A. D. Hamilton, *Tetrahedron* **55**, 6027–6038 (1999).
- <sup>26</sup>S. Lotze and H. Bakker, *J. Chem. Phys.* **142**, 212436 (2015).
- <sup>27</sup>A. Huerta-Viga *et al.*, “Structure of a salt bridge stabilizing a  $\beta$ -turn in water and DMSO” (unpublished).
- <sup>28</sup>A. Huerta-Viga, D. J. Shaw, and S. Woutersen, *J. Phys. Chem. B* **114**, 15212–15220 (2010).
- <sup>29</sup>M. J. Frisch *et al.*, GAUSSIAN 09, Revision D.01, Gaussian Inc., Wallingford, CT, 2009.
- <sup>30</sup>A. Huerta-Viga, S. R. Domingos, S. Amirjalayer, and S. Woutersen, *Phys. Chem. Chem. Phys.* **16**, 15784–15786 (2014).
- <sup>31</sup>A. Barth, *Prog. Biophys. Mol. Biol.* **74**, 141–173 (2000).
- <sup>32</sup>A. Ghosh, M. J. Tucker, and R. M. Hochstrasser, *J. Phys. Chem. A* **115**, 9731–9738 (2011).
- <sup>33</sup>See supplementary material at <http://dx.doi.org/10.1063/1.4921064> for additional information, figures, and tables that are referenced in the main text.
- <sup>34</sup>S. Woutersen and P. Hamm, *J. Chem. Phys.* **114**, 2727–2737 (2001).
- <sup>35</sup>R. Mayer and G. Lancelot, *J. Am. Chem. Soc.* **103**, 4738–4742 (1981).
- <sup>36</sup>B. M. Huyghues-Despointes, J. M. Scholtz, and R. L. Baldwin, *Protein Sci.* **2**, 80–85 (1993).
- <sup>37</sup>S. Krimm and J. Bandekar, *Adv. Protein Chem.* **38**, 181–364 (1986).
- <sup>38</sup>A. Lupas, *Trends Biochem. Sci.* **21**, 375–382 (1996).
- <sup>39</sup>D. A. D. Parry, R. D. B. Fraser, and J. M. Squire, *J. Struct. Biol.* **163**, 258–269 (2008).
- <sup>40</sup>B. Apostolovic, M. Danial, and H.-A. Klok, *Chem. Soc. Rev.* **39**, 3541–3575 (2010).
- <sup>41</sup>P. Burkhard, M. Meier, and A. Lustig, *Protein Sci.* **9**, 2294–2301 (2000).
- <sup>42</sup>I. T. Arkin, *Curr. Opin. Chem. Biol.* **10**, 394–401 (2006).
- <sup>43</sup>P. Hamm and M. Zanni, *Concepts and Methods of 2D Infrared Spectroscopy*, 1st ed. (Cambridge University Press, 2011).